This article has been accepted for publication in a future issue of this journal, but has not been fully edited. Content may change prior to final publication. Citation information: DOI 10.1109/TVT.2017.2729346, IEEE Transactions on Vehicular Technology

Capacity- and Trust-aware BS Cooperation in Non-uniform HetNets: Spectral Efficiency and Optimal BS Density

Huici Wu, *Student Member, IEEE,* Ning Zhang, *Member, IEEE,* Xiaofeng Tao, *Senior Member, IEEE,* Zhiqing Wei, *Member, IEEE,* and Xuemin (Sherman) Shen, *Fellow, IEEE*

***Abstract*—This paper studies base station (BS) cooperation in non-uniform heterogeneous networks (HetNets). Considering the limited capacity at BS and existence of untrusted small cell base stations (SBSs) in practical scenarios, a novel capacity- and trust-aware BS cooperation strategy is proposed. The BS cooperation is performed in a user centric manner, based on the average received signal strength at users, the capacity of BSs, and the trustworthiness of SBSs. Furthermore, with the proposed BS cooperation, the statistics of aggregate information-signal strength and interference strength are theoretically analyzed, based on stochastic geometry. Then, expressions for spectral efficiency (SE) and area spectral efficiency (ASE) are analytically derived. In addition, to study the impact of the SBS density on the SE and ASE, the optimal densities of normal SBSs to maximize the SE and ASE are proved to exist and obtained. Finally, simulations and numerical evaluations validate the theoretical analysis and reveal that (i) with the awareness of BS capacity and trustworthiness, optimal cooperative thresholds achieving the maximum SE and ASE exist, which decrease with high path-loss exponent; and (ii) in high path-loss fading environment with high existence probability of untrusted SBSs, more normal SBSs are required to be deployed to achieve the maximum SE and ASE performance.**

***Index Terms*—BS cooperation, optimal BS density, HetNets, stochastic geometry**

I. Introduction

With proliferation of connected wireless devices (e.g., smart phones, tablets, connected vehicles [1], etc.) and emergence of diverse wireless services (e.g., video streaming, social networking, etc.), mobile data will dramatically increase. It is predicted that the overall mobile data traffic generated by these devices will grow to 30.6 exabytes per month by 2020, which is an eightfold increase over 2015 [2]. Next generation (5G) wireless networks expect to accommodate such a mobile data surge, through three main technical aspects: spectrum extension, spectrum efficiency enhancement, and network densification [3]–[6]. As the dominant theme in 5G, network densification is to densely deploy diverse small cell base stations (SBSs) coexisting with conventional macro base stations (MBSs), giving rise to heterogeneous networks (HetNets).

The HetNet architecture, making mobile terminals closer to access points (APs) or BSs, can not only improve network coverage and capacity, but also provide higher spectrum efficiency. However, it also poses many technical challenges, such as resource/interference management, mobility management, security, etc. The resulting interference, including inter-tier interference and intra-tier interference, is one of the top technical challenges that severely deteriorate the performance of HetNets. To cope with the severe interference in HetNets, Coordinated Multi Point (CoMP) transmission, either in the form of multi-node joint transmission (JT) [7]–[9] or coordinated scheduling and coordinated beamforming (CS/CB) [10], [11], has been acknowledged as a promising technique in coor-

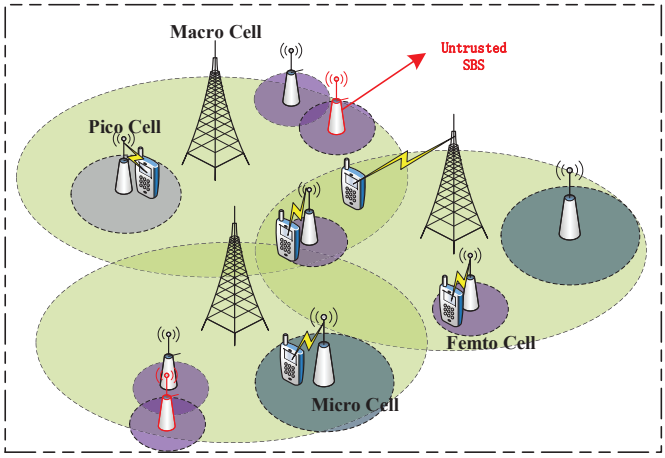

Fig. 1. An illustration of heterogeneous networks with untrusted SBSs. The macro BSs are overlaid by three tiers of low-power BSs and APs in the same geographic area. Untrusted SBSs may exist in the proximity of normal SBSs.

Manuscript received November 17, 2016; accepted July 13, 2017. This work was supported in part by the National Natural Science Foundation for Distinguished Young Scholars of China under Grant 61325006, in part by the National Natural Science Foundation of China (No. 61231009, No. 61601055), in part by the 111 Project of China under the Grant B16006, and in part by the Natural Sciences and Engineering Research Council of Canada. The associate editor coordinating the review of this paper and approving it for publication was Honggang Wang. *Corresponding author: Xiaofeng Tao*

H. Wu and X. Tao are with the National Engineering Lab for Mobile Network Technologies, Beijing University of Posts and Telecommunications, Beijing 100876, China (e-mail: {dailywu, taoxf}@bupt.edu.cn).

Z. Wei is with the Wireless Technology Innovation (WTI) Institute, Beijing University of Posts and Telecommunications, Beijing 100876, China (e-mail: weizhiqing@bupt.edu.cn).

N. Zhang is with the Department of Computing Science at Texas A&M University-Corpus Christi (e-mail: Ning.Zhang@tamucc.edu).

X. Shen is with the Department of Electrical and Computer Engineering, University of Waterloo, Waterloo, ON N2L 3G1, Canada (e-mail: sshen@uwaterloo.ca).

This article has been accepted for publication in a future issue of this journal, but has not been fully edited. Content may change prior to final publication. Citation information: DOI 10.1109/TVT.2017.2729346, IEEE Transactions on Vehicular Technology

dinating small cell BSs and macro BSs to mitigate interference and further improve the performance and efficiency of the network.

A. Related Work and Motivation

In literatures, joint transmission with multiple nodes across tiers in HetNets has been investigated either by removing the dominant interferers [12], [13] or transforming the interferers to joint transmitters [14]–[19]. The performance analysis of joint transmission is significant for providing theoretical guidance and insights to practical operation of HetNets. Stochastic geometry has been widely applied in modeling the distribution of wireless nodes in HetNets, where the BSs in different tiers are modeled as independent homogeneous Poisson Point Processes (PPPs). The existing works have also developed tractable results to characterize the statistics of interference and signal-to-interference-and-noise ratio (SINR) in HetNets with various BS cooperation strategies.

The SINR distribution with noncoherent joint-transmission (NC-JT) BS cooperation was studied in a homogeneous (single-tier) wireless cellular network [14]. A cooperative BS joins to transmit the user's data only if the instantaneous received-signal-strength (RSS) on the corresponding link is above a given threshold. The same cooperation strategy was also investigated in a K-tier HetNet in [15], where spectral efficiency (SE) for the typical user was derived. [16] investigated the performance of JT and CB with quantized and delayed channel state information (CSI). An adaptive multi-mode transmission scheme was proposed, which switches between JT and CB to maximize the data rate. In [17], a location-aware BS cooperation scheme was proposed in a two-tier HetNet to enhance the performance of the users suffering from high cross-tier interference. Outage probability, achievable data rate and load per BS were analyzed. A multi-cell cooperation scheme was proposed to improve the coverage performance of cell-edge users in our prior work [18], where the coverage probability of a randomly located user was derived. A general BS cooperation across tiers was proposed and analyzed in [19]. K tiers of BSs are sorted in an increasing order by long-term average RSS and a typical user connects to the n strongest BSs. General expressions for coverage probability, diversity gain and power gain are derived. Following their contributions, Gaurav studied spatio-temporal cooperation in HetNets [12], where the cooperative transmission was extended to simultaneous multi-BS cooperation and retransmission at a cooperative BS. Two cooperation strategies including joint transmission and BS silencing were investigated and expressions for coverage probabilities were provided. Note that the studies on BS cooperation in the aforementioned literatures are assumed with light-loaded BSs, which does not consider the impact of the practical BS load on the BS cooperation and the system performance.

On the other hand, although BS cooperation can provide better coverage and capacity performance in HetNets, distributing the information signal of mobile users to multiple cooperative BSs may cause information leakage due to the development of large-scale, distributed, ever more open and diverse architecture of HetNets [20]. Since SBSs can be deployed by users, the adversaries can easily deploy their SBSs, making the network more vulnerable to eavesdropping and attacks. Moreover, these SBSs are usually deployed in cluster manner, like in stadium, mall and etc, which makes the information security problem more severe since the illegal access points such as pseudo BSs are much easier to mask themselves and act as regular BSs among the clusters, as depicted in Fig. 1. These illegal nodes can lunch different attacks such as man-in-the-middle attack (MITM) [21], denial-of-service (DoS) attack [22], replay attack and eavesdropping, etc. These attacks may cause disable or information leakage of wireless transmissions. For example, in the man-in-the-middle attack (also known as fire brigade attacks), the attacker access to the communication channel between two end terminals and control over the end-users confidential message. DoS attacks make the network resources unavailable to the end users and the replay attacks cause ambiguous information transmission. Therefore, the trustworthiness and security status of BSs and access points should be considered into the BS cooperation to guarantee the information security in wireless communications.

To sum up, the main factors for BS cooperation in practical systems: i) the limited capacity of BSs, and ii) the trustworthiness of SBSs, are rarely considered in existing literatures. Specifically, the BSs were usually considered to be capable of serving any number of users during cooperation, which is not reasonable in practice due to the densely deployment of SBSs in HetNets and the scarcity of frequency and spatial resources. Thus, the BS capacity, i.e., the maximum number of mobile terminals that can be associated with a BS, is limited in practice. In addition, the SBSs are not always trusted in practical deployment since the SBSs could be compromised or easily deployed by malicious users with illegal purpose. Moreover, to make a efficient attack, especially eavesdropping attack, the untrusted SBSs are always deployed around the legitimate transmitter. Therefore, it is of great importance to address those issues to harvest the benefits of BS cooperation in practical systems.

B. Contribution and Organization

In this paper, considering the limited capacity and trustworthiness of BSs, we propose a capacity- and trust-aware BS cooperation strategy in the non-uniform HetNets. Two tiers of HetNet including trusted MBSs and partly trusted SBSs is studied, where Gaussian Poisson Process (GPP) is applied to model the cluster property of SBSs and the existence of the untrusted SBSs. All the BSs are equipped with multiple antennas and can simultaneously serve multiple users in a time-frequency channel. The BSs participate in cooperation in a user-centric manner and the mobile users can adaptively update the cooperation BS cluster according to their service requirement and actual network status, including the trustworthiness of BSs and the traffic load of BSs. In a nutshell, the contribution of this paper is summarized as follows.

- We propose a capacity- and trust-aware BS cooperation scheme performing in a user centric way, whereby different BSs are selected to cooperatively serve users,

This article has been accepted for publication in a future issue of this journal, but has not been fully edited. Content may change prior to final publication. Citation information: DOI 10.1109/TVT.2017.2729346, IEEE Transactions on Vehicular Technology

based on the received signal power from potential BSs at users, the capacity of BSs, and the trustworthiness of SBSs. Furthermore, we theoretically analyzed the spectral efficiency (SE) and area spectral efficiency (ASE) with stochastic geometry.

- The optimal SBS densities that maximize the SE and ASE are proved to exist and obtained. The analyses show that the optimal SBS density maximizing the ASE is denser than that maximizing the SE.
- Extensive simulation results are provided to validate the theoretical analysis and to show the impact of the system parameters on the SE and ASE performance. The results indicate that i) with the awareness of BS capacity and trustworthiness, there exist optimal cooperative thresholds for the determination of cooperative BSs to achieve the best SE and ASE performance, and lower optimal cooperative thresholds are needed with higher path-loss exponent; ii) more normal SBSs can be deployed in high path-loss fading environments to achieve the best SE and ASE performance; and iii) larger distance repulsion between BSs can provide better SE and ASE performance when the area for candidate cooperative is too large or too small. Moreover, small distance repulsion can provide better performance with the optimal cooperative threshold.

The reminder of this paper is organized as follows. The system model, the proposed BS cooperation strategy and mathematical preliminaries are presented in Section II. In Section III, expressions of SE and ASE for the proposed BS cooperation strategy are analytically derived. Then, the existence of optimal small BS densities maximizing the SE and ASE are proved and the optimal SBS densities are provided in Section IV. Simulation results are given in Section V. Finally, Section VI concludes this paper.

Notation: Lower case characters are used for vectors. Detailed notations are summarized as in Table I.

TABLE I
NOTATIONS SUMMARY

Symbol	Description
$\Phi_1\left(\lambda_1\right) \in \mathbb{R}^2$	PPP model of MBSs with density λ_1
$\Phi_g\left(\lambda_g\right) \in \mathbb{R}^2$	GPP model of all SBSs (normal and untrusted SBS) with density λ_g
$\Phi_2\left(\lambda_2\right) \in \mathbb{R}^2$	PPP model of normal SBSs with density λ_2
P_1^{tx}, P_2^{tx}	Transmit power of MBS and SBS
N_1, N_2	Number of antennas at MBS and SBS
K_1, K_2	Capacity of MBS and SBS
q	Existence probability of untrusted SBSs
α	Path-loss exponent
$\Gamma\left(x,y\right)$, $\gamma\left(x,y\right)$	Upper and lower incomplete gamma function
$\mathcal{B}\left(o,r\right)$	Circular area centered at o and with radius r
$\mathbb{1}\left(*\right)$	Indicator function with value 1 if the event $*$ is true, and 0, otherwise.

II. System Model and Mathematical Preliminary

In this section, the system model, including spatial model of wireless nodes and the proposed BS cooperation strategy, will be firstly described. Then, the definition of GPP will be presented.

A. System model and the proposed BS cooperation strategy

Downlink transmission in a two-tier HetNet is considered, where BSs are equiped with multiple antennas. Each MBS and SBS is equipped with N_1 and N_2 antennas, and serves at most K_1 ($K_1 \leqslant N_1$) and K_2 ($K_2 \leqslant N_2$) users at a resource block, respectively. Single omni-antenna is equipped at mobile users. The transmit power at MBS and SBS are fixed as P_1^{tx} and P_2^{tx}, respectively. In this paper, we mainly focus on the BS cooperation in a reference channel.

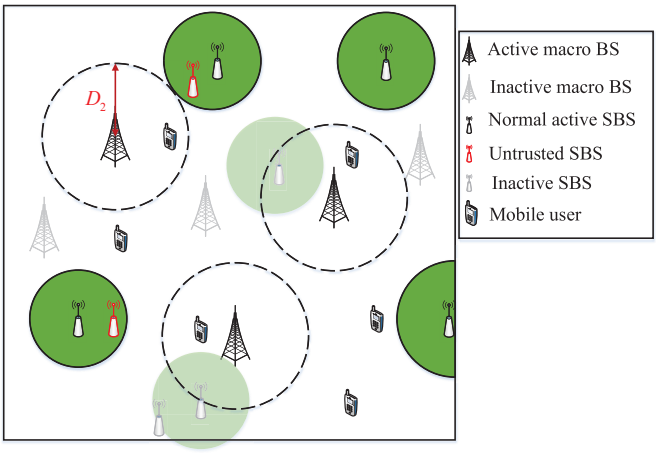

Fig. 2. Two-tier HetNets with untrusted SBSs.

*1) **Distribution of BS and mobile users**:* The distribution of MBSs are modeled as a two-dimensional homogeneous PPP $\Phi_1 \in \mathbb{R}^2$ with spatial density λ_1. Consider the intra-tier repulsion among BSs, a MBS is not retained if there are any other MBSs located around it. Specifically, if any other MBSs are located in a circle area centered at the MBS with radius D_1, i.e., located inside $\mathcal{B}\left(MBS, D_1\right)$, the MBS will be removed, as depicted in Fig. 2. Then, for an arbitrary MBS, it retains in the process with probability

$$\upsilon_1 = \frac{1 - e^{-\pi D_1^2 \lambda_1}}{\pi D_1^2 \lambda_1} \tag{1}$$

and all the retained MBSs can be approximated as a reformulated PPP $\Phi_1^{'} \in \mathbb{R}^2$ with thinning density $\lambda_1^{'} = \lambda_1 \upsilon_1$ [23], [24].

Normal SBSs and untrusted SBSs are considered. The normal SBSs are distributed according to a PPP $\Phi_2 \in \mathbb{R}^2$ with density λ_2. To model the existence of untrusted SBSs, we assume that an untrusted SBS exists near a normal SBS with probability q and the distance between untrusted SBS and normal SBS follows some certain distribution. As a result, the distribution of all SBSs, including normal SBSs and untrusted SBSs, are formulated as a Gaussian-Poisson Point Process $\Phi_g \in \mathbb{R}^2$, with spatial density λ_2 of the parent process $\Phi_2 \in \mathbb{R}^2$. In the GPP model, one or two points are included in a cluster. If there is only one point, then the point is considered to be normal SBS. If there are two points (referred to as a couple), the point at the position of parent PPP is considered to be normal SBS while the other is untrusted SBS. The untrusted SBS can eavesdrop or attack

This article has been accepted for publication in a future issue of this journal, but has not been fully edited. Content may change prior to final publication. Citation information: DOI 10.1109/TVT.2017.2729346, IEEE Transactions on Vehicular Technology

the confidential messages transmitted by its couple or interrupt the transmission.

Considering the inter-tier repulsion between MBSs and SBSs, those SBSs with cluster center located inside the circular area of any active MBSs will be removed. We define the circular area of MBSs as interference protection area (dotted circle in Fig. 2) and the radius of the protection area is D_2. Mathematically, an arbitrary SBS cluster retains if the distance between the cluster center and its nearest active MBS is greater than D_2. Also, we define the minimum intra-tier distance repulsion between any SBSs as D_3. Thus an SBS cluster retains with probability $\upsilon_2 = e^{-\pi D_2^2 \lambda_1^{'} \frac{1-e^{-\pi D_3^2 \lambda_2}}{\pi D_3^2 \lambda_2}}$. All the retained SBS clusters can be approximated as a re-formed GPP $\Phi_g^{'} \in \mathbb{R}^2$ with parent process $\Phi_2^{'} \in \mathbb{R}^2$ of density $\lambda_2^{'} = \lambda_2 \upsilon_2$.

Mobile users are distributed according to another independent homogeneous PPP $\Phi_u \in \mathbb{R}^2$ with density λ_u. Without loss of generality, a reference user, viewed as a typical user, is located at the origin of the coordinate plane [25].

*2) **The proposed capacity- and trust-aware BS cooperation strategy**:* Perfect CSI[1] is assumed to be well known at BSs, e.g., through pilot training. Both path-loss fading $l(d) = d^{-\alpha}$ and block Rayleigh fading with unit mean are considered as signal propagation, where d is the distance between the transmit-receive pair and α ($\alpha > 2$) is path-loss exponent. Moreover, Zero-forcing (ZF) is adopted at the BSs to serve multiple users simultaneously, with low complexity and fairly good performance [26], [27]. BS cooperation is performed in a user centric way, whereby different BSs across tiers are selected to cooperatively serve the mobile users, based on the average received signal power of the corresponding link, the capacity of BSs, and the trustworthiness of SBSs. Specifically, since all the MBSs are trusted, an MBS participates in the cooperation if

- the MBS is not full-loaded, and
- the average RSS at mobile users from the MBS is greater than a predetermined cooperative threshold τ_1,

For the SBSs, the untrusted SBSs are not allowed to participate in cooperation and a normal SBSs will joint to transmit the users' data if

- the normal SBSs are in security state, i.e., i) only one SBS in a cluster, or ii) two SBS in a cluster but the untrusted SBS is located outside the normal SBS's security area, where the average RSS at the untrusted SBS (from its couple) is below a security threshold τ_3.
- the normal SBS is not full-loaded, and
- the average RSS at mobile users from the normal SBS is greater than a predetermined cooperative threshold τ_2.

Note that when the load of a BS exceeds its capacity, the BS will be congested and serving requests sending by mobile users may be blocked. Moreover, the cooperation condition of the average RSS not only guarantee the effectiveness of the signal propagation, but also restricts the geographical area for the cooperative BSs and hence reduces the implementation overhead of BS selection.

[1]We assume perfect CSI in this paper to investigate the fundamental insights into the BS cooperation in HetNet. Imperfect CSI will be studied as our future work.

Remark: Location information of untrusted BS is assumed to be known in this work. When the untrusted SBSs are active points, such as an active relay or a pseudo BS sending scam signals, the average RSS can be evaluated at the normal SBS in a cluster by collecting the statistical information. For example, statistical analyzing the signaling characteristics and accounting the area where the pseudo-base station frequently update their Location Area Code (LAC) can determine the approximated location of the pseudo-base station. Then, real-time monitoring can position the pseudo-base station. In such a way, the average RSS can be evaluated. When the untrusted SBSs are silent points, the channel state information can also be acquired based on the observation that the untrusted SBS will use a local oscillator to perform base-band conversion of the signal from normal SBS, and a known impairment of oscillators is that part of the generated sinusoidal tone back-propagates to the antenna ports and leaks out [28]. This signal can be detected by the SBSs in the cluster and used for average RSS estimation purposes.

B. Gaussian-Poisson Point Process

The GPP is a Poisson cluster process with homogeneous independent clusters. One point or two points are contained in a cluster with probability $1-q$ and q, respectively. If a cluster has one point, it is located at the center of the cluster. If a cluster has two points, then one of the points is located at the center of the cluster and the other one is randomly distributed around the center with random distance. Mathematically, the GPP can be expressed as $\Phi_g = \bigcup_{y \in \Phi_2} \Phi_y$, where $\Phi_2 = \{y_1, y_2, ...\}$ is the parent process of the GPP and $\{\Phi_y, y \in \Phi_2\}$ denotes the cluster centered at y. More specifically, $\{\Phi_y\}$ can be expressed as:

$$\Phi_y = \begin{cases} \{y\}, 1-q \\ \{y, y+z_y\}, q \end{cases} \tag{2}$$

where $\{z_y\} \in \mathbb{R}^2$ are identically and independently distributed with Gamma distributed inter-point distance $\|z_x\|$ as in [29]. The probability density function (*pdf*) of $\|z_x\|$ is denoted as $\|z_x\| \sim \text{Gamma}(\kappa, \theta)$ with parameter κ and θ . Thus, the density of the GPP is $\lambda_g = \lambda_2 (1+q)$.

III. SE and ASE Analysis

In this section, SE and ASE are used as the performance metrics to evaluate the proposed BS cooperation strategy. The SE is defined as the average data rate per frequency bandwidth achievable at a randomly located user and the ASE, average data per frequency bandwidth in a unit area, is defined to measure the average throughput of the HetNet. In the following, the distribution of BS load is firstly analyzed. Then, the received SINR at the typical user is presented, and the SE and ASE are analyzed, based on the statistics of aggregate information-signal strength and interference strength.

A. Statistics of BS load

Denote by ρ_{1,k_1} the probability that $k_1 \leqslant K_1$ users are associated with an arbitrary MBS located at x within a

This article has been accepted for publication in a future issue of this journal, but has not been fully edited. Content may change prior to final publication. Citation information: DOI 10.1109/TVT.2017.2729346, IEEE Transactions on Vehicular Technology

resource block, then with BS cooperation strategy for MBSs, ρ_{1,k_1} is expressed as

$$\rho_{1,k_1}=\begin{cases}\text{Prob}\left\{k_1 \text{ mobile users with RSS } \geqslant \tau_1\right\}, k_1<K_1\\ \sum\limits_{k=K_1}^{\infty}\text{Prob}\left\{k \text{ mobile users with RSS } \geqslant \tau_1\right\}, k_1=K_1\end{cases}$$
$$=\begin{cases}\text{Prob}\left\{k_1 \text{ mobile users inside } \mathcal{B}\left(x,\chi_1\right)\right\}, k_1<K_1\\ \sum\limits_{k=K_1}^{\infty}\text{Prob}\left\{k \text{ mobile users inside } \mathcal{B}\left(x,\chi_1\right)\right\}, k_1=K_1\end{cases}$$
$$\overset{(a)}{=}\begin{cases}\frac{\left(\pi\lambda_u\chi_1^2\right)^{k_1}\exp\left(-\pi\lambda_u\chi_1^2\right)}{k_1!}, k_1<K_1\\ \sum\limits_{k=K_1}^{\infty}\frac{\left(\pi\lambda_u\chi_1^2\right)^{k}\exp\left(-\pi\lambda_u\chi_1^2\right)}{k!}, k_1=K_1\end{cases}$$
$$=\begin{cases}\frac{\left(\pi\lambda_u\chi_1^2\right)^{k_1}\exp\left(-\pi\lambda_u\chi_1^2\right)}{k_1!}, k_1<K_1\\ \frac{\gamma\left(K_1,\pi\lambda_u\chi_1^2\right)}{K_1!}, k_1=K_1\end{cases} \tag{3}$$

where *(a)* follows the PPP of mobile users. $\chi_1=\left(\frac{P_1^{tx}}{\tau_1}\right)^{1/\alpha}$ is the radius for cooperative MBSs and $\gamma\left(x,y\right)=\int_0^y t^{x-1}e^{-t}dt$ is lower incomplete gamma function. Similarly, denote by ρ_{2,k_2} the probability that $k_2\leqslant K_2$ users are associated with an arbitraty normal SBS located at y within a time slot. For simplicity, we denote E_1 as the event that only one normal SBS is in a cluster, E_2 as the event that two SBSs are in a cluster, and E_3 as the event that the untrusted SBSs is out of the security area. Then the probabilities that events E_1, E_2 and E_3 occur are respectively given as follows.

$$\text{Prob}\left\{E_1\right\}=1-q, \text{Prob}\left\{E_2\right\}=q \tag{4}$$

$$\text{Prob}\left\{E_3\right\}=\text{Prob}\left\{\text{Received RSS at the couple}\leqslant\tau_3\right\}$$
$$=\text{Prob}\left\{P_2^{tx}\|z_y\|^{-\alpha}<\tau_3\right\}=\frac{\Gamma\left(\kappa,\frac{\chi_3}{\theta}\right)}{\Gamma\left(\kappa\right)}\triangleq\eta, \tag{5}$$

where $\chi_3=\left(\frac{P_2^{tx}}{\tau_3}\right)^{\frac{1}{\alpha}}$ is the minimum radius for the security area. $\Gamma\left(x,y\right)=1-\gamma\left(x,y\right)$ is the upper incomplete gamma function. As a result, when a normal SBS is not in security state, the normal SBS is zero-loaded with probability $q\left(1-\eta\right)$. Otherwise, a normal SBS is in security state with probability $\left(1-q+q\eta\right)$. And the load distribution ρ_{2,k_2^y} of an secure SBS can be expressed as:

$$\rho_{2,k_2}=\begin{cases}\text{Prob}\left\{k_2 \text{ mobile users inside } \mathcal{B}\left(y,\chi_2\right)\right\}, k_2<K_2\\ \sum\limits_{k=K_2}^{\infty}\text{Prob}\left\{k \text{ mobile users inside } \mathcal{B}\left(y,\chi_2\right)\right\}, k_2=K_2\end{cases}$$
$$=\begin{cases}\frac{\left(\pi\lambda_u\chi_2^2\right)^{k_2}\exp\left(-\pi\lambda_u\chi_2^2\right)}{k_2!}, k_2<K_2\\ \frac{\gamma\left(K_2,\pi\lambda_u\chi_2^2\right)}{K_2!}, k_2=K_2\end{cases} \tag{6}$$

where $\chi_2=\left(\frac{P_2^{tx}}{\tau_2}\right)^{1/\alpha}$ is the minimum radius of the area for cooperative SBSs.

B. Received Signal-to-Interference-plus-Noise Ratio

With the proposed BS cooperation, mobile users not only receive information signals from cooperative serving BSs, but also suffer from inter-tier and intra-tier interference from all the other BSs except the serving BSs. The resulting links from cooperative BSs and interfering BSs to the mobile users are multiple-user multiple-input single-output (MU-MISO) channels. Noncoherent joint transmission[2] is employed at the cooperative BSs as in [14], [15] and equal power allocation is adopted. The received SINR at the typical user is thus given as

$$\gamma=\frac{S_m+S_s}{I_m+I_s+\sigma^2} \tag{7}$$

where σ^2 is white noise power and

$$S_m=\sum_{x\in\Phi_1'\cap\mathcal{B}(0,\chi_1)}\mathbb{1}\left(k_1^x<K_1\right)\frac{P_1^{tx}}{k_1^x+1}\|x\|^{-\alpha}h_x \tag{8}$$

is the aggregate information-signal strength from cooperative MBSs. $\mathbb{1}\left(k_1^x<K_1\right)$ is indicator function defined such that $\mathbb{1}\left(k_1^x<K_1\right)=1$ if the MBS located at x is not full-loaded, and $\mathbb{1}\left(k_1^x<K_1\right)=0$, otherwise. S_s is the aggregate information-signal strength from the cooperative SBSs.

$$S_s=\sum_{y\in\Phi_2'\cap\mathcal{B}(0,\chi_2)}\mathbb{1}\left(k_2^y<K_2\right)\mathbb{1}\left(E_1 \text{ or } \left(E_2\&E_3\right)\right)\frac{P_2^{tx}}{k_2^y+1}\|y\|^{-\alpha}h_y \tag{9}$$

where $\mathbb{1}\left(E_1 \text{ or } \left(E_2\&E_3\right)\right)$ is indicator function indicating that the normal SBSs located at y is in security state. For the aggregate interference I_m, since the interfering MBSs include MBSs inside $\mathcal{B}\left(o,\chi_1\right)$ and outside $\mathcal{B}\left(o,\chi_1\right)$, I_m can be expressed as:

$$\begin{aligned}I_m&=I_{m,in}+I_{m,out}\\&=\sum_{x'\in\Phi_1'\cap\mathcal{B}(0,\chi_1)}\mathbb{1}\left(k_1^{x'}=K_1\right)\frac{P_1^{tx}}{k_1^{x'}}\left\|x'\right\|^{-\alpha}h_{x'}\\&+\sum_{x'\in\Phi_1'\setminus\mathcal{B}(0,\chi_1)}\mathbb{1}\left(k_1^{x'}>0\right)\frac{P_1^{tx}}{k_1^{x'}}\left\|x'\right\|^{-\alpha}h_{x'}\end{aligned} \tag{10}$$

where $I_{m,in}$ is the aggregate interference caused by MBSs inside $\mathcal{B}\left(o,\chi_1\right)$ and $I_{m,out}$ is the aggregate interference caused by MBSs outside $\mathcal{B}\left(o,\chi_1\right)$. Similarly, the interfering SBSs include SBSs inside $\mathcal{B}\left(o,\chi_2\right)$ and outside $\mathcal{B}\left(o,\chi_2\right)$ and the aggregate interference I_s can be expressed as:

$$\begin{aligned}I_s&=I_{s,in}+I_{s,out}\\&=\sum_{y'\in\Phi_2'\cap\mathcal{B}(0,\chi_2)}\left(\begin{aligned}&\mathbb{1}\left(k_2^{y'}=K_2\right)\mathbb{1}\left(E_2\&E_3\right)\frac{P_2^{tx}}{k_2^{y'}}\|y\|^{-\alpha}h_{y'}+\\&\mathbb{1}\left(0<k_2^{y'}<K_2\right)\mathbb{1}\left(E_2\&!E_3\right)\frac{P_2^{tx}}{k_2^{y'}}\left\|y'\right\|^{-\alpha}h_{y'}\end{aligned}\right)\\&+\sum_{y'\in\Phi_2'\setminus\mathcal{B}(0,\chi_2)}\mathbb{1}\left(k_2^{y'}>0\right)\frac{P_2^{tx}}{k_2^{y'}}\left\|y'\right\|^{-\alpha}h_{y'}\end{aligned} \tag{11}$$

where $!E_3$ is the opposite event of E_3, i.e., the event that the untrusted SBSs is inside the security area. Notice that the untrusted SBSs will not actively transmit signals to any mobile users, and thus they will not interfere with any communication links.

From the system model, ZF precoding is adopted at BSs. Thus, if a MBS x cooperates to serve the typical user, the

[2]As stated in [14], noncoherent cooperation outperforms its coherent counterpart due to less stringent synchronization and CSI requirements

This article has been accepted for publication in a future issue of this journal, but has not been fully edited. Content may change prior to final publication. Citation information: DOI 10.1109/TVT.2017.2729346, IEEE Transactions on Vehicular Technology

small-scale fading h_x is gamma distributed with parameters $N_1 - k_1^x$ and 1, i.e., $h_x \sim \text{Gamma}\left(N_1 - k_1^x, 1\right)$ [26], [30]. If a MBS $x^{'}$ does not cooperate to serve the typical user, $h_{x^{'}}$ is approximated as gamma distribution with parameters k_1^x and 1, i.e., $h_{x^{'}} \sim \text{Gamma}\left(k_1^{x^{'}}, 1\right)$ [27], [31]. Similarly, h_y and $h_{y^{'}}$ are gamma distributions, $h_y \sim \text{Gamma}\left(N_2 - k_2^y, 1\right)$, $h_{y^{'}} \sim \text{Gamma}\left(k_2^{y^{'}}, 1\right)$.

C. Spectral Efficiency

Adopting appropriate adaptive modulation and coding, the spectral efficiency achievable at the typical user is

$$\mathcal{R}_c = \mathbb{E}\left[\ln\left(1 + \frac{S_m + S_s}{I_m + I_s + \sigma^2}\right)\right] \text{(nats/s/Hz)} \tag{12}$$

where the expectation is taken average over the statistics of information-signal strength and interference strength, which considers the effect of BS capacity and trustworthiness of SBSs. Denote by $\rho_1 = [\rho_{1,0}, \rho_{1,1}, ..., \rho_{1,K_1}]$ and $\rho_2 = [\rho_{2,0}, \rho_{2,1}, ..., \rho_{2,K_2}]$ the vectors of the BS load at MBSs and SBSs, respectively. Then, the SE is analytically derived as in the following theorem.

Theorem 1. *With the awareness of BS capacity and trustworthiness, the spectral efficiency with the proposed BS cooperation strategy in the MU-MISO non-uniform HetNets is approximated as*

$$\begin{aligned}\mathcal{R}_c \approx \int_0^\infty & \exp\left\{-\lambda_1 u_1(t) - \lambda_2 u_2(t)\right\} \\ & \times \left\{1 - \exp\left\{-\lambda_1 w_1(t) - \lambda_2 w_2(t)\right\}\right\} \frac{e^{-\sigma^2 t}}{t} dt\end{aligned} \tag{13}$$

where

$$u_i(t) = \pi \upsilon_i a_i \begin{bmatrix} \chi_i^2 \rho_{i,K_i}\left(1 - \mathcal{Z}\left(K_i, \frac{t\tau_i}{K_i}\right)\right) \\ + \left(tP_i^{tx}\right)^{2/\alpha} \psi\left(K_i, \rho_i, t\tau_i\right) \end{bmatrix}, \tag{14}$$

$$w_i(t) = \pi \upsilon_i a_i \chi_i^2 \sum_{k_i=0}^{K_i - 1} \rho_{i,k_i}\left(1 - \mathcal{Z}\left(N_i - k_i, \frac{t\tau_i}{k_i + 1}\right)\right) \tag{15}$$

with

$$\psi(a, \mathbf{b}, x) = \frac{2}{\alpha} \sum_{k=1}^{a} b_k \int_{x^{-1}}^\infty \left(1 - \frac{(kv)^k}{(kv+1)^k}\right) v^{\frac{2}{\alpha} - 1} dv, \tag{16}$$

$$\mathcal{Z}(b, x) = \frac{2x^{-b}}{\alpha b + 2} \times {}_2F_1\left(b, b + \frac{2}{\alpha}; b + 1 + \frac{2}{\alpha}; -\frac{1}{x}\right). \tag{17}$$

and $a_1 = 1, a_2 = 1 - q + q\eta$.

Proof: Please refer to the detailed proof in Appendix A. ∎

Although Eq. (13) is in an integral form, $\psi(a, \mathbf{b}, x)$ and $\mathcal{Z}(b, x)$ can be easily calculated by Matlab, and therefore $\mathcal{R}_c$ can be numerically evaluated by applying Monte Carlo integration methods. Compared with existing literatures, expression (13) reflects BS load and security state of small BSs.

D. Area Spectral Efficiency

The ASE is applied as a metric to measure the network throughput in a unit area. The average mobile users associated with a MBS and a normal SBS are given as

$$\overline{\mathcal{K}_1} = \sum_{k_1=1}^{K_1} \rho_{1,k} k_1, \overline{\mathcal{K}_2} = (1 - q + q\eta) \sum_{k_2=1}^{K_2} \rho_{2,k} k_2 \tag{18}$$

For a sufficient large area $\mathcal{S}$, the average network throughput per unit area, i.e., ASE, with the proposed BS cooperation strategy is

$$ASE = \frac{\left(\mathcal{S}\lambda_1^{'}\overline{\mathcal{K}_1} + \mathcal{S}\lambda_2^{'}\overline{\mathcal{K}_2}\right)\mathcal{R}_c}{\mathcal{S}} = \left(\lambda_1^{'}\overline{\mathcal{K}_1} + \lambda_2^{'}\overline{\mathcal{K}_2}\right)\mathcal{R}_c \tag{19}$$

for which the unit is nats/s/Hz/m^2.

From (13) and (19), the path-loss exponent α, the existence probability of untrusted SBSs (q), the density of trusted BSs (λ_1 and λ_2), and the distance repulsion among BSs have great impact on the SE and ASE performance.

Since the normal SBSs reuse the spectrum resources of MBSs, the density of normal SBSs (i.e., λ_2) has great impact on the SE and ASE performance. When λ_2 is below a certain value, the enhancement of information-signal strength is greater than the increase of interference strength with denser SBSs. This is caused by the fact that the propagation of information signals transform from non-line-of-sight (NLOS) to line-of-sight (LOS) with the denser of SBSs, while the propagation of interference signals are still dominated by NLOS. With increasing λ_2, the increase of interference strength will dominate the increase of information-signal strength. As a result, the system performance will be firstly improved and then deteriorated over λ_2. To exploit the impact of the deployment of normal SBSs, we study the optimization problem for the density of normal SBSs in the following section.

IV. Optimization of SBS Density

Inter-tier and intra-tier interferences in HetNets deteriorate system performance severely. MBSs, well-planed by operators, are always assumed to be deployed with fixed density. While the low-power SBSs are deployed by operators and costumers according to connectivity and traffic demands. Appropriately increasing the deployment of SBSs can improve network capacity and coverage for both mobile users and the overall network. However, these performance may degrade with the increasing of SBS density due to the sharp increase of interference[3]. Hence, in this section, we prove the existence of the optimal λ_2 and provide expressions for the optimal densities.

Differentiating (13) with respect to λ_2, we have

$$\frac{d\mathcal{R}_c}{d\lambda_2} = \int_0^\infty f(t, \lambda_2) \frac{e^{-\sigma^2 t}}{t} dt \tag{20}$$

[3]As for fixed transmit power at SBSs, the interference increases sharply and the system performance, like coverage and network capacity, deteriorates. We focus on the SBS density optimization in this paper and will study the influence of SBS density with the varying of transmit power in the future.

This article has been accepted for publication in a future issue of this journal, but has not been fully edited. Content may change prior to final publication. Citation information: DOI 10.1109/TVT.2017.2729346, IEEE Transactions on Vehicular Technology

where $f(t,\lambda_2)$ is shown as

$$\begin{aligned} & f(t,\lambda_2) \\ &= \frac{d}{d\lambda_2}\begin{pmatrix} \exp\{-\lambda_1 u_1(t)-\lambda_2 u_2(t)\} \\ \times\{1-\exp\{-\lambda_1 w_1(t)-\lambda_2 w_2(t)\}\} \end{pmatrix} \\ &= \exp\{-\lambda_1 w_1(t)\}(u_2(t)+w_2(t)) \\ &\times \exp\{-\lambda_2(u_2(t)+w_2(t))-\lambda_1 u_1(t)\} \\ &-u_2(t)\exp\{-\lambda_2 u_2(t)-\lambda_1 u_1(t)\} \end{aligned} \tag{21}$$

Defining the function $g(z)=ze^{-\lambda_2 z-\lambda_1 u_1(t)}$, then $f(t,\lambda_2)$ can be re-expressed as

$$f(t,\lambda_2)=\exp\{-\lambda_1 w_1(t)\}\, g(u_2(t)+w_2(t))-g(u_2(t)) \tag{22}$$

To prove the existence of the optimal normal SBS density, we prove

1) $\frac{d\mathcal{R}_c}{d\lambda_2}=0$ has a unique solution λ_2^*, and
2) $\frac{d\mathcal{R}_c}{d\lambda_2}>0$ when $\lambda_2<\lambda_2^*$ and $\frac{d\mathcal{R}_c}{d\lambda_2}<0$ when $\lambda_2>\lambda_2^*$.

In the following, we provide the theorem and corresponding proof for the existence of optimal λ_2 that maximizes the spectral efficiency.

Theorem 2. *With the awareness of BS capacity and trustworthiness, optimal normal SBS density exists such that the spectral efficiency with the proposed BS cooperation strategy is maximized. In addition, the optimal λ_2 is the solution of the following equation.*

$$\int_0^\infty \{\exp[-\lambda_1 w_1(t)]\, g(u_2(t)+w_2(t)) - g(u_2(t))\}\frac{e^{-\sigma^2 t}}{t}dt=0 \tag{23}$$

Proof: With the definition of $g(z)$, it satisfies $g'(z)>0$ when $z<\frac{1}{\lambda_2}$, and $g'(z)\leqslant 0$ when $z\geqslant\frac{1}{\lambda_2}$, which is a unimodal function with a unique maximum value at $z^*=\frac{1}{\lambda_2}$. With variable $0<a\leqslant 1$ and a positive y, there always exist an $z^*=\frac{ay}{e^{\lambda_2 y}-a}$ satisfying the following inequality.

- When $z<z^*$, $\frac{ag(z+y)}{g(z)}>1$, i.e., $ag(z+y)-g(z)>0$
- When $z>z^*$, $\frac{ag(z+y)}{g(z)}<1$, i.e., $ag(z+y)-g(z)<0$

An illustration of function $g(z)$ is depicted as in Fig. 3.

Since $u_i(t)$ and $w_i(t)$ are increasing functions of t and $0<\exp\{-\lambda_1 w_1(t)\}\leqslant 1$, there always exists $u_i^*(t^*)$ and $w_i^*(t^*)$ with t^*, satisfying the following inequality.

- When $t<t^*$, $f(t,\lambda_2)>0$
- When $t>t^*$, $f(t,\lambda_2)<0$

Thus, the integral function (20) starts with a positive value, which is increasing when the upper limit of integral is below t^* and decreasing when the upper limit of integral is above t^*. Function $g(z)$ states that z^* decreases with increasing of λ_2. Since $u_i(t)$ and $w_i(t)$ are increasing function of t, t^* decreases with λ_2. As a result, $\frac{d\mathcal{R}_c}{d\lambda_2}$ is a decreasing function of λ_2. On the other hand, $g(u_2(t)+w_2(t))$ and $g(u_2(t))$ state that $t^n\propto\frac{c}{\lambda_2}$ with a certain n. Thus, $\lim t^*\to\infty$ with $\lim\lambda_2\to 0$, and $\frac{d\mathcal{R}_c}{d\lambda_2}>0$ hold. Moreover, since

$$\lim_{\lambda_2\to\infty}\frac{\exp\{-\lambda_1 w_1(t)\}\, g(u_2(t)+w_2(t))}{g(u_2(t))}=0, \tag{24}$$

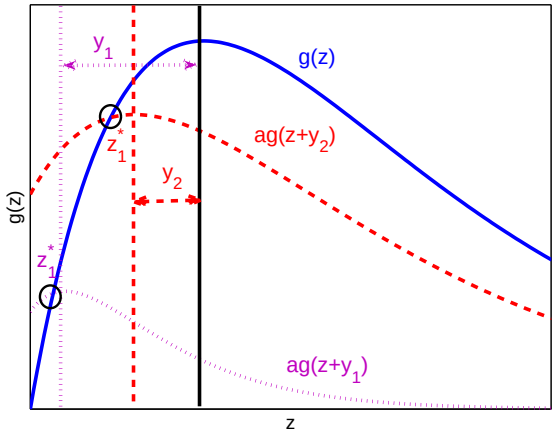

Fig. 3. An illustration of Function $g(z)$

we have $\lim_{\lambda_2\to\infty} f(t,\lambda_2)<0,\forall t$ and

$$\lim_{\lambda_2\to\infty}\frac{d\mathcal{R}_c}{d\lambda_2}=\lim_{\lambda_2\to\infty}\int_0^\infty f(t,\lambda_2)\frac{e^{-\sigma^2 t}}{t}dt<0 \tag{25}$$

holds.

Finally, sum up the above discussions as in Table II[4]. It is concluded that the unique optimal value for λ_2 exists and can be obtained by solving the equation $\frac{d\mathcal{R}_c}{d\lambda_2}=0$. ■

TABLE II
TREND OF VARIABLES AND FUNCTIONS

λ_2	t^*	$f(t,\lambda_2)$	$\frac{d\mathcal{R}_c}{d\lambda_2}$
$\to 0$	$\to\infty$	\	>0
$\uparrow$	$\downarrow$	\	$\downarrow$
$\to\infty$	$\to 0$	<0	<0

Similarly, we prove the existence of the optimal λ_2 that maximizes the ASE with the proposed BS cooperation scheme.

Corollary 1. *In the MU-MISO non-uniform HetNets with the proposed BS cooperation strategy, there exists optimal normal SBS density maximizing the ASE performance, and the optimal value of the SBS density can be obtained by setting (26) to zero.*

Proof: Differentiating (19) with respect to λ_2, we have

$$\frac{dASE}{d\lambda_2}=\overline{\mathcal{K}_2}\upsilon_2\mathcal{R}_c+\left(\lambda_1'\overline{\mathcal{K}_1}+\lambda_2'\overline{\mathcal{K}_2}\right)\frac{d\mathcal{R}_c}{d\lambda_2}. \tag{26}$$

Since $0\leqslant\overline{\mathcal{K}_2}\upsilon_2\mathcal{R}_c\leqslant+\infty$, combining (25) and Table II, we can conclude that the ASE is an upper unimodal function and the unique optimal SBS density can be obtained by setting (26) to zero. ■

Combining Eq. (20) and (26), since $\overline{\mathcal{K}_2}\upsilon_2\mathcal{R}_c\geqslant 0$ and $\lambda_1'\overline{\mathcal{K}_1}+\lambda_2'\overline{\mathcal{K}_2}\geqslant 0$, the optimal normal SBS density maximizing the ASE is denser than that maximizing the SE.

[4] ↑ means increasing and ↓ means decreasing.

This article has been accepted for publication in a future issue of this journal, but has not been fully edited. Content may change prior to final publication. Citation information: DOI 10.1109/TVT.2017.2729346, IEEE Transactions on Vehicular Technology

V. Simulation Results

In this section, simulation results and numerical results are provided to validate the theoretical analyses and provide some insights in the MU-MISO HetNets with the proposed BS cooperation scheme. The detailed system parameters are given in Table. III unless otherwise specified. The simulation results are obtained through 10^4 times Monte Carlo simulations in a circular area with radius 10km. For each spatial realization, the MBSs and SBSs are randomly distributed according to homogeneous PPPs and are deactivated with the distance repulsion between MBSs and SBSs. An SINR sample is obtained by generating independent Rayleigh random vectors for the fading channels.

TABLE III
Parameters used in the simulations

Parameters	Value
Density of MBS, the parent process of SBS and mobile user. (λ_1, λ_2 and λ_u)	$\frac{1}{\pi 500^2}$, $\frac{5}{\pi 500^2}$, $\frac{5}{\pi 500^2}$
Number of antennas at MBS and SBS	$N_1 = 8$, $N_2 = 4$
Capacity at MBS and SBS	$K_1 = 8$, $K_2 = 4$
Transmit power at MBS and SBS	$P_1^{\text{tx}} = 37$dBm, $P_2^{\text{tx}} = 30$dBm
Parameters for Gamma distribution of inter-point distance	$\kappa = 25$, $\theta = 2$
Thermal noise σ^2 (10MHz bandwidth)	$\sigma^2 = -104$dBm

Figs. 4-8 show the comparison of the analytical results and the simulation results. The gap between the simulation results and the analytical results is due to the PPP approximation of the retained MBSs and SBSs. However, the gap is quite small, which verifies the accuracy of the PPP approximation and the derived theoretical expressions. Furthermore, Fig. 4-6 show the SE and ASE with respect to the cooperative thresholds τ_1 and τ_2 with different distance repulsions. Firstly, different cooperative threshold τ_2 and path-loss exponent α are analyzed in Fig. 4. It can be seen that optimal cooperative thresholds always exist such that the maximum SE and maximum ASE can be achieved. The reason mainly lies in the fact that with the limited capacity of BSs, severe congestion will occur when the cooperative thresholds are lower than some certain values. In such cases, the average probabilities for a mobile user to get served, i.e., Prob $(k_1^x < K_1)$ and Prob $(k_2^y < K_2)$, are almost zero and the SE will be near zero. With the increasing of cooperative thresholds, there will be less congestion and Prob $(k_1^x < K_1)$ and Prob $(k_2^y < K_2)$ increases. However, the number of BSs that can provide services for a mobile user decreases as cooperative thresholds rise. As a result, there will exist optimal cooperative thresholds balancing the serving probability and number of cooperative BSs, which determine the best SE and ASE performance. Moreover, low path-loss exponent results in high optimal cooperative threshold τ_1.

Fig. 5 and Fig. 6 show the effect of distance repulsions D_1, D_2 and D_3. Form these two figures, we can see that when the cooperative thresholds τ_1 and τ_2 are small, the BSs are almost full-loaded with probability 1 and thus the BSs can not participate in cooperation but they interferer with the typical user. Therefore, a larger distance repulsion between BSs can deactivate more BSs and provide better SE performance but deteriorate the overall network performance, i.e., the ASE.

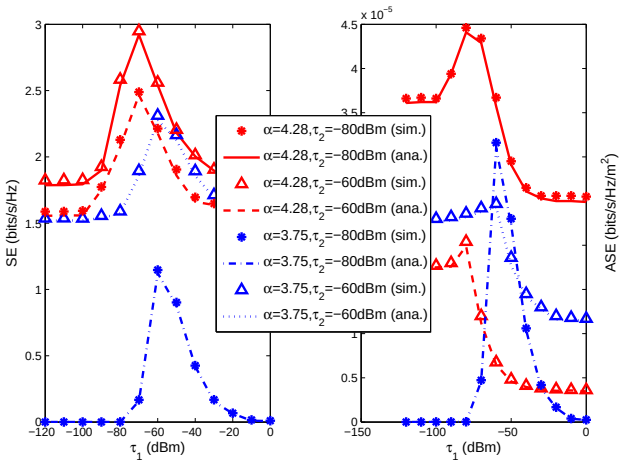

Fig. 4. SE and ASE with respect to cooperative threshold τ_1 for different path-loss exponents and cooperative thresholdτ_2 ($q = 0.5$, $D_1 = 400$m, $D_2 = 100$m, $D_3 = 20$m, $\tau_3 = -45$dBm).

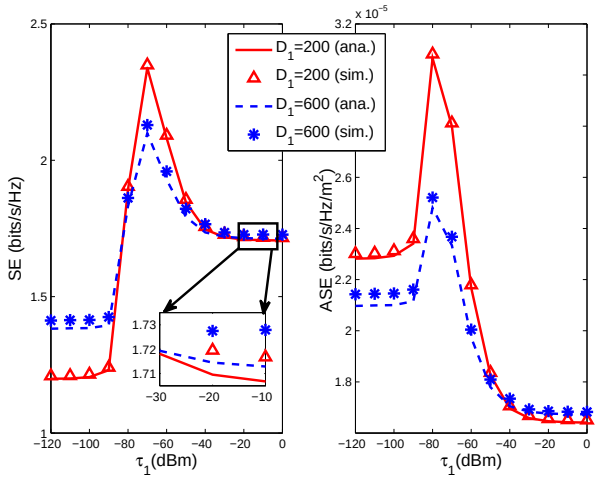

Fig. 5. SE and ASE with respect to τ_1 ($\alpha = 4.28$, $q = 0.5$, $D_2 = 100$m, $D_3 = 20$m, $\tau_2 = -80$dBm, $\tau_3 = -45$dBm).

With the increasing of τ_1 and τ_2, the loads at BSs are relaxed and more BSs can participate in cooperation to further improve the system performance. As a result, reducing the distance repulsion D_1 and D_2 can retain more BSs and provide better SE and ASE performance. However, with the increasing of τ_1, the number of MBSs as well as the MBS load are reduced and finally no MBS will cooperate to serve the typical user. In such a scenario, a larger distance repulsion D_1 can make the MBS more sparse and thus more SBSs can be retained to have the opportunity to participate in cooperation. Besides, we can see from Fig. 6 that the intra-tier distance repulsion between SBSs has little influence on the SE and ASE performance.

The existence of untrusted SBSs greatly influences the selection of cooperative SBSs and thus affects the system performance. Fig. 7 shows the SE and ASE with respect to the existence probability of untrusted SBSs q for different security threshold τ_3. The average probability that the untrusted SBSs is out of the security area is $\eta \approx 1$ when $\tau_3 = -35$dBm

This article has been accepted for publication in a future issue of this journal, but has not been fully edited. Content may change prior to final publication. Citation information: DOI 10.1109/TVT.2017.2729346, IEEE Transactions on Vehicular Technology

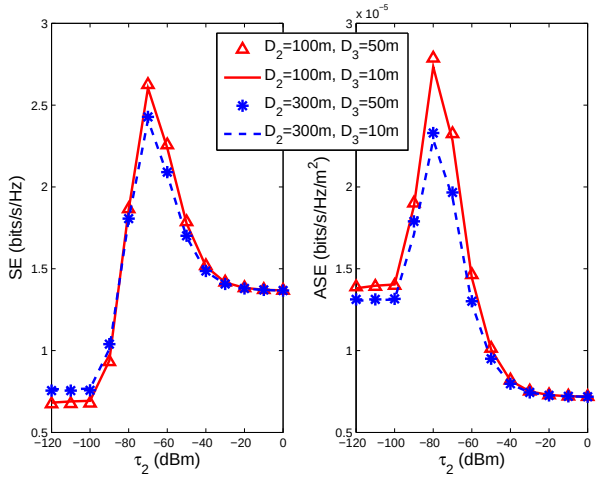

Fig. 6. SE and ASE with respect to τ_2 ($\alpha = 4.28$, $q = 0.5$, $D_1 = 400$m $\tau_1 = -80$dBm, $\tau_3 = -45$dBm).

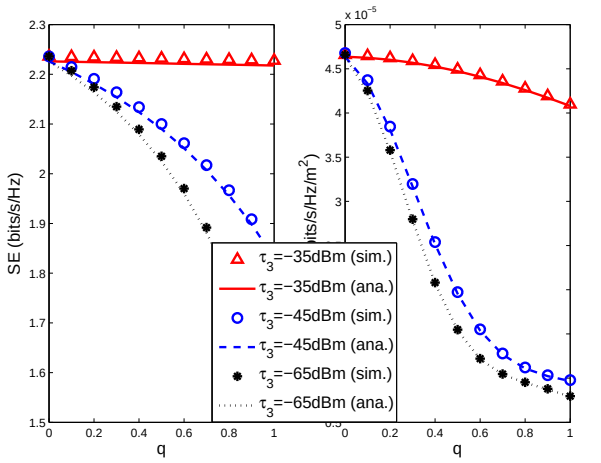

Fig. 7. SE and ASE with respect to q ($\alpha = 4.28$, $D_1 = 400$m, $D_2 = 100$m, $D_3 = 20$m, $\tau_1 = -80$dBm, $\tau_2 = -80$dBm).

and $\eta \approx 0$ when $\tau_3 = -65$dBm. $\eta \approx 1$ means that all the normal SBSs are in security state and can provide secure data transmission for mobile users. In such a case, the existence probability of untrusted SBSs does not influence the SE and ASE performance. $\eta \approx 0$ means that all the normal SBSs in a cluster containing two SBSs are not in security state and cannot cooperate to transmit user's data. In such a case, the average number normal SBSs that can participate in the cooperation decreases over q and the SE and ASE performance deteriorate with the existence probability of untrusted SBSs.

Fig. 8 shows the impact of the density of normal SBSs. It can be seen that the SE and ASE are unimodal functions with λ_2, which numerically validates Theorem. 2 and Corollary 1. Moreover, it can also be seen that the optimal λ_2 with a high path-loss exponent is greater than that with a small path-loss exponent, and a larger path-loss exponent provides higher SE and ASE. This result indicates that, to achieve the best SE and ASE performance, more normal SBSs should be deployed in high path-loss fading environments. Also, better

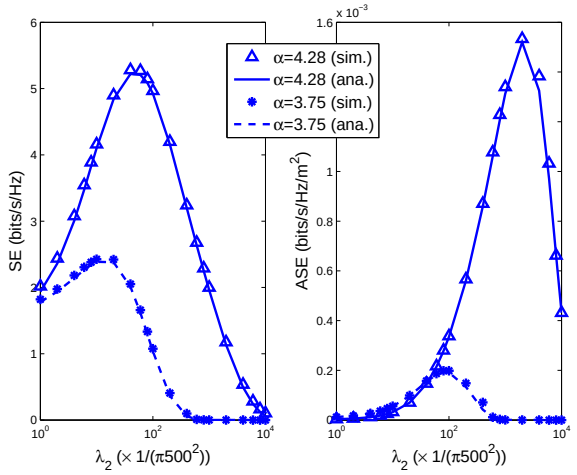

Fig. 8. SE and ASE with respect to λ_2 ($q = 0.5$, $\tau_1 = -65$dBm, $\tau_2 = -65$dBm, $\tau_3 = -35$dBm).

system performance can be achieved in high path-loss fading environment.

Fig. 9 and Fig. 10 show the optimal normal SBS density and the corresponding SE and ASE with respect to the cooperative threshold τ_2 for different path-loss exponent α and existence probability of untrusted SBSs q, respectively. From Fig. 9, it can be seen that the optimal λ_2 increases with the cooperative threshold τ_2, which is caused by the fact that denser SBSs are needed to achieve the maximum SE and ASE when the area for cooperative BSs shrinks. Moreover, higher optimal SBS density is needed with larger q and the optimal λ_2 maximizing ASE is greater than that maximizing SE with the same cooperative thresholds. Fig. 10 shows that there is an optimal cooperative threshold τ_2 such that the SE and ASE are maximized. In addition, a lower cooperative threshold is desired in wireless environments with higher path-loss fading, which is the same to the results obtained in Fig. 4. In addition, the maximum SE and ASE do not change with the existence probability of untrusted SBSs because the existence of untrusted SBSs only influences the density of the normal SBSs in secure status. As a result, to achieve the same density of secure normal SBSs, more normal SBSs are needed with high existence probability of untrusted SBSs.

VI. Conclusion

In this paper, a capacity- and trust-aware BS cooperation strategy has been proposed for the MU-MISO non-uniform HetNets. Closed-form expressions for spectral efficiency and area spectral efficiency have been analytically obtained with the proposed cooperation scheme. Furthermore, optimal densities of normal SBSs maximizing the SE and ASE have been proved to exist and derived. The proposed BS cooperation strategy can be employed in practical systems, where capacity of BSs are limited and not all SBSs are trusted. Simulation results have validated the theoretical analysis and demonstrated that there also exist optimal cooperative thresholds for determination of cooperative BSs to maximize the SE and ASE. Moreover, to achieve the maximum SE and ASE

This article has been accepted for publication in a future issue of this journal, but has not been fully edited. Content may change prior to final publication. Citation information: DOI 10.1109/TVT.2017.2729346, IEEE Transactions on Vehicular Technology

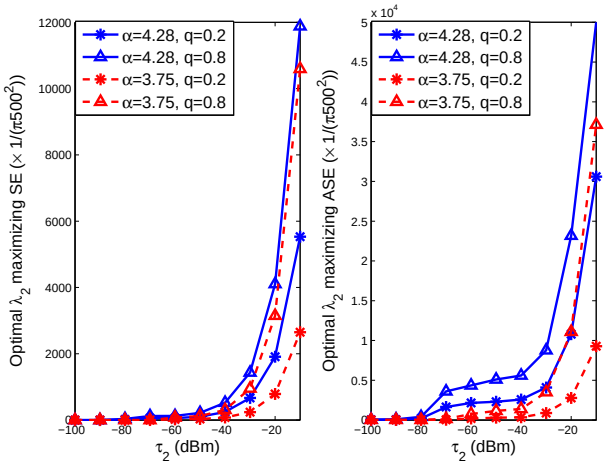

Fig. 9. Optimal density of untrusted small BSs with respect to τ_2 ($D_1 = 400$m, $D_2 = 100$m, $D_3 = 20$m, $\tau_1 = -60$dBm, $\tau_3 = -45$dBm).

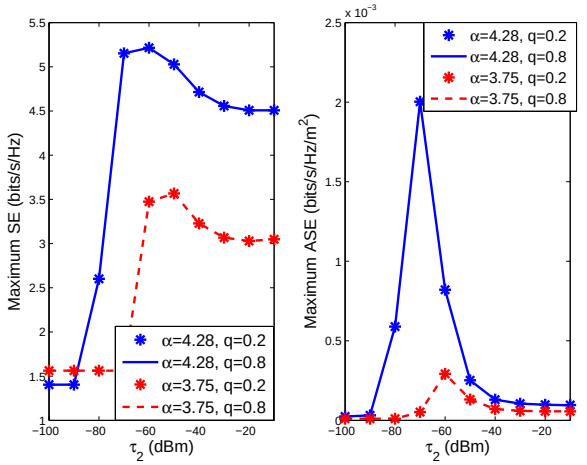

Fig. 10. The corresponding maximum SE and ASE.

performance, lower cooperative thresholds are required and more normal SBS are needed to deployed in the high path-loss fading environments. Besides, for the scenario with a high probability of the existence of untrusted SBSs, more normal SBSs are required to achieve the best SE and ASE.

For the future work, we will investigate BS cooperation, when reputation based scheme [32] is adopted to monitor and manage the trustworthiness of SBSs. Interested readers can refer to [33], [34] for a general overview of the reputation based system. In addition, cooperation among SBSs with energy harvesting will also be studied, where the dynamic energy status of SBSs should be considered when performing cooperation.

APPENDIX A
PROOF OF THEOREM 1

Before we analyze the spectral efficiency, a useful lemma is presented as follow.

Lemma 1. *Let* $x_1, ..., x_N$, $y_1, ..., y_M$ *be arbitrary non-negative random variables. Setting* $x = \sum_{n=1}^{N} x_n$ *and* $y = \sum_{m=1}^{M} y_m$, *then*

$$\mathbb{E}\left[\ln\left(1+\frac{x}{1+y}\right)\right] = \int_0^\infty \frac{\mathcal{L}_y(t) - \mathcal{L}_{y+x}(t)}{t} e^{-t} dt \quad (27)$$

where $\mathcal{L}_A(t) = \mathbb{E}\left[e^{-tA}\right]$ *is the Laplace function of random variable* A.

Proof: Detailed proof can be referred to in [35]. ■

With Lemma 1, the SE of a typical user is

$$\begin{aligned}\mathcal{R}_c &\overset{(c)}{=} \int_0^\infty \frac{\mathcal{L}_{I_m+I_s}(t)\left(1-\mathcal{L}_{S_m+S_s}(t)\right)}{t} e^{-\sigma^2 t} dt \\ &\overset{(d)}{\approx} \int_0^\infty \frac{\mathcal{L}_{I_m}(t)\mathcal{L}_{I_s}(t)\left(1-\mathcal{L}_{S_m}(t)\mathcal{L}_{S_s}(t)\right)}{t} e^{-\sigma^2 t} dt\end{aligned} \quad (28)$$

where *(c)* holds due to the independence between information power and interference power and *(d)* is the result of the independence between the retained MBSs and SBSs in the approximated PPPs. Related with the Laplace functional of point processes, the Laplace transform of variable S_m can be calculated as

$$\begin{aligned}&\mathcal{L}_{S_m}(t) = \mathbb{E}_{S_m}\left[e^{-tS_m}\right] \\ &= \mathbb{E}_{\Phi_1', h_x}\left[\prod_{x\in\Phi_1'\cap\mathcal{B}(0,\chi_1)} e^{-\mathbb{1}(k_1^x<K_1) t \frac{P_1^{tx}}{k_1^x+1}\|x\|^{-\alpha} h_x}\right] \\ &\overset{(e)}{=} \exp\left\{-2\pi\lambda_1' \int_0^{\chi_1}\left(1-\mathbb{E}_h\left[e^{-\mathbb{1}(k_1<K_1) t \frac{P_1^{tx}}{k_1+1} r^{-\alpha} h}\right]\right) r dr\right\} \\ &\overset{(f)}{=} \exp\left\{-2\pi\lambda_1' \int_0^{\chi_1}\left(1-\rho_{1,K_1}-\sum_{k_1=0}^{K_1-1}\rho_{1,k_1}\mathbb{E}_h\left[e^{-t\frac{P_1^{tx}}{k_1+1} r^{-\alpha} h}\right]\right) r dr\right\}\end{aligned} \quad (29)$$

where *(e)* follows the probability generating functional (PGFL) of PPP [25] and *(f)* follows the distribution of k_1 and index $\mathbb{1}(k_1 < K_1)$. Since $h \sim$ Gamma$(N_1 - k_1, 1)$, $\mathbb{E}_h\left[e^{-\frac{tP_1^{tx}}{k_1+1} r^{-\alpha} h}\right]$ is derived as

$$\mathbb{E}_h\left[e^{-\frac{tP_1^{tx}}{k_1+1} r^{-\alpha} h}\right] = \left(1+\frac{tP_1^{tx}}{k_1+1} r^{-\alpha}\right)^{-(N_1-k_1)}$$

This article has been accepted for publication in a future issue of this journal, but has not been fully edited. Content may change prior to final publication. Citation information: DOI 10.1109/TVT.2017.2729346, IEEE Transactions on Vehicular Technology

Then, $\mathcal{L}_{S_m}(t)$ can be re-written as

$$\mathcal{L}_{S_m}(t)=\exp\left\{\begin{array}{l}-2\pi\lambda_1^{'}\left[(1-\rho_{1,K_1})\int_0^{\chi_1}rdr-\right.\\ \left.\sum_{k_1=0}^{K_1-1}\int_0^{\chi_1}\frac{\rho_{1,k_1}}{\left(1+t\frac{P_1^{tx}}{k_1+1}r^{-\alpha}\right)^{(N_1-k_1)}}rdr\right]\end{array}\right\}$$

$$\overset{(g)}{=}\exp\left\{\begin{array}{l}-\pi\lambda_1^{'}\left[(1-\rho_{1,K_1})\chi_1^2-\sum_{k_1=0}^{K_1-1}\rho_{1,k_1}\left(\frac{tP_1^{tx}}{k_1+1}\right)^{2/\alpha}\right.\\ \left.\times\int_0^{\left(\frac{t\tau_1}{k_1+1}\right)^{-2/\alpha}}\frac{u^{\frac{\alpha}{2}(N_1-k_1)}}{\left(1+u^{\frac{\alpha}{2}}\right)^{(N_1-k_1)}}du\right]\end{array}\right\} \quad (30)$$

$$\overset{(h)}{=}\exp\left\{\begin{array}{l}-\pi\lambda_1^{'}\left[(1-\rho_{1,K_1})\chi_1^2-\sum_{k_1=0}^{K_1-1}\frac{2\rho_{1,k_1}(tP_1^{tx})^{2/\alpha}}{(k_1+1)^{2/\alpha}\alpha}\right.\\ \left.\times\int_0^{\frac{k_1+1}{t\tau_1}}\frac{v^{\frac{2}{\alpha}+(N_1-k_1)-1}}{(1+v)^{(N_1-k_1)}}dv\right]\end{array}\right\}$$

$$\overset{(i)}{=}\exp\left\{-\pi\lambda_1^{'}\chi_1^2\sum_{k_1=0}^{K_1-1}\rho_{1,k_1}\left(1-\mathcal{Z}\left(N_1-k_1,\frac{t\tau_1}{k_1+1}\right)\right)\right\} \quad (31)$$

where *(g)* and *(h)* are obtained by replacing $u=\left(\frac{tP_1^{tx}}{k_1+1}\right)^{-2/\alpha}r^2$ and $v=u^{\frac{\alpha}{2}}$, respectively. *(i)* is derived by applying Eq. (3.194/2) in [36].

Similarly, with (9), the Laplace transform of S_s is

$$\mathcal{L}_{S_s}(t)=\mathbb{E}_{S_s}\left[e^{-tS_s}\right]$$

$$=\exp\left\{\begin{array}{l}-2\pi\lambda_2^{'}\int_0^{\chi_2}[1-\\ \mathbb{E}_h\left[e^{-\mathbf{1}(k_2<K_2)\mathbf{1}(E_1\text{ or }(E_2\&E_3))t\frac{P_2^{tx}}{k_2+1}r^{-\alpha}h}\right]\end{array}\right\}rdr$$

$$\overset{(j)}{=}\exp\left\{\begin{array}{l}-2\pi\lambda_2^{'}\int_0^{\chi_2}[1-(\rho_{2,K_2}+(1-\rho_{2,K_2})q(1-\eta))\\ -a_2\sum_{k_2=0}^{K_2-1}\rho_{2,k_2}\mathbb{E}_h\left[e^{-t\frac{P_2^{tx}}{k_2+1}r^{-\alpha}h}\right]rdr\end{array}\right\}$$

$$\overset{(k)}{=}\exp\left\{\begin{array}{l}-2\pi\lambda_2^{'}a_2\times\\ \sum_{k_2=0}^{K_2-1}\rho_{2,k_2}\int_0^{\chi_2}\left(1-\frac{1}{\left(1+t\frac{P_2^{tx}}{k_2+1}r^{-\alpha}\right)^{(N_2-k_2)}}\right)rdr\end{array}\right\}$$

$$=\exp\left\{-\pi\lambda_2^{'}\chi_2^2a_2\sum_{k_2=0}^{K_2-1}\rho_{2,k_2}\left(1-\mathcal{Z}\left(N_2-k_2,\frac{t\tau_2}{k_2+1}\right)\right)\right\} \quad (32)$$

where *(j)* holds due to the fact that a normal SBS does cooperate to transmit users' data with probability $\rho_{2,K_2}+(1-\rho_{2,K_2})q(1-\eta)$ and the corresponding $\mathbb{E}_h\left[e^{-t\frac{P_2^{tx}}{k_2+1}r^{-\alpha}h}\right]=1$. $a_2=1-q+q\eta$ is the probability that the normal SBS in a cluster is in security state. *(k)* is the result from the Gamma distribution of h, i.e., $h_y\sim$ Gamma$(N_2-k_2^y,1)$.

Since the aggregate interference generated by MBSs inside $\mathcal{B}(o,\chi_1)$ and outside $\mathcal{B}(o,\chi_1)$ are independent, the Laplace transform of interference power I_m can be calculated as

$$\mathcal{L}_{I_m}(t)=\mathbb{E}_{I_{m,in}}\left[e^{-tI_{m,in}}\right]\mathbb{E}_{I_{m,out}}\left[e^{-tI_{m,out}}\right] \quad (33)$$

where $\mathbb{E}_{I_{m,in}}\left[e^{-tI_{m,in}}\right]$ is derived as

$$\mathbb{E}_{I_{m,in}}\left[e^{-tI_{m,in}}\right]$$

$$=\mathbb{E}_{\Phi_1^{'},h_{x^{'}}}\left[e^{-t\sum_{x^{'}\in\Phi_1^{'}\cap\mathcal{B}(0,\chi_1)}\mathbb{1}\left(k_1^{x^{'}}=K_1\right)\frac{P_1^{tx}}{k_1^{x^{'}}}\left\|x^{'}\right\|^{-\alpha}h_{x^{'}}}\right]$$

$$=\exp\left\{\begin{array}{l}-2\pi\lambda_1^{'}\int_0^{\chi_1}[1-\\ \left(\left(\rho_{1,K_1}\mathbb{E}_h\left[e^{-t\frac{P_1^{tx}}{K_1}r^{-\alpha}h}\right]+1-\rho_{1,K_1}\right)\right)rdr\end{array}\right\}$$

$$\overset{(l)}{=}\exp\left\{-2\pi\lambda_1^{'}\int_0^{\chi_1}\left(\rho_{1,K_1}-\frac{\rho_{1,K_1}}{\left(1+t\frac{P_1^{tx}}{K_1}r^{-\alpha}\right)^{K_1}}\right)rdr\right\}$$

$$=\exp\left\{-\pi\lambda_1^{'}\chi_1^2\rho_{1,K_1}\left(1-\mathcal{Z}\left(K_1,\frac{t\tau_1}{K_1}\right)\right)\right\}, \quad (34)$$

and $\mathbb{E}_{I_{m,out}}\left[e^{-tI_{m,out}}\right]$ is

$$\mathbb{E}_{I_{m,out}}\left[e^{-tI_{m,out}}\right]$$

$$=\mathbb{E}_{\Phi_1^{'},h_{x^{'}}}\left[e^{-t\sum_{x^{'}\in\Phi_1^{'}\setminus\mathcal{B}(0,\chi_1)}\mathbb{1}\left(k_1^{x^{'}}>0\right)\frac{P_1^{tx}}{k_1^{x^{'}}}\left\|x^{'}\right\|^{-\alpha}h_{x^{'}}}\right]$$

$$=\exp\left\{-2\pi\lambda_1^{'}\int_{\chi_1}^{\infty}\left(1-\rho_{1,0}-\sum_{k_1=1}^{K_1}\rho_{1,k_1}\mathbb{E}_{h^{'}}\left[e^{-t\frac{P_1^{tx}}{k_1}r^{-\alpha}h^{'}}\right]\right)rdr\right\}$$

$$\overset{(l)}{=}\exp\left\{-2\pi\lambda_1^{'}\int_{\chi_1}^{\infty}\left(\sum_{k_1=1}^{K_1}\rho_{1,k_1}\left(1-\frac{1}{\left(1+t\frac{P_1^{tx}}{k_1}r^{-\alpha}\right)^{k_1}}\right)\right)rdr\right\}$$

$$=\exp\left\{-\pi\lambda_1^{'}\left(tP_1^{tx}\right)^{2/\alpha}\psi\left(K_1,\rho_{1,*},t\tau_1\right)\right\}. \quad (35)$$

(l) is the result from $h_{x^{'}}\sim$ Gamma$\left(k_1^{x^{'}},1\right)$.

Similarly, the Laplace transform of I_s can be obtained as $\mathcal{L}_{I_s}(t)=\mathbb{E}_{I_{s,in}}\left[e^{-tI_{s,in}}\right]\mathbb{E}_{I_{s,out}}\left[e^{-tI_{s,out}}\right]$, where

$$\mathbb{E}_{I_{s,in}}\left[e^{-tI_{s,in}}\right]$$

$$=\exp\left\{\begin{array}{l}-2\pi\lambda_2^{'}\int_0^{\chi_2}\left[1-(1-q+q\eta)\sum_{k_2=1}^{K_2-1}\rho_{2,k_2}-q(1-\eta)\right.\\ \left.-(1-q+q\eta)\rho_{2,K_2}\mathbb{E}_h\left[e^{-t\frac{P_2^{tx}}{K_2}r^{-\alpha}h}\right]rdr\right.\end{array}\right\}$$

$$=\exp\left\{-\pi\lambda_2^{'}\chi_2^2(1-q+q\eta)\rho_{2,K_2}\left(1-\mathcal{Z}\left(K_2,\frac{t\tau_2}{K_2}\right)\right)\right\} \quad (36)$$

This article has been accepted for publication in a future issue of this journal, but has not been fully edited. Content may change prior to final publication. Citation information: DOI 10.1109/TVT.2017.2729346, IEEE Transactions on Vehicular Technology

and

$$\begin{aligned}&\mathbb{E}_{I_{s,out}}\left[e^{-tI_{s,out}}\right]\\&=\exp\left\{-2\pi\lambda_2^{'}\int_{\chi_2}^{\infty}\left(1-\mathbb{E}_{h'}\left[e^{-\mathbb{1}\left(k_2^{y'}>0\right)t\frac{P_2^{tx}}{k_2^{y}}r^{-\alpha}h'}\right]\right)rdr\right\}\\&=\exp\left\{-\pi\lambda_2^{'}(1-q+q\eta)\left(tP_2^{tx}\right)^{2/\alpha}\psi\left(K_2,\rho_{2,*},t\tau_2\right)\right\}\end{aligned} \tag{37}$$

Substituting (31), (32) and (34)-(37) into (28), (13) for spectral efficiency is proved.

ACKNOWLEDGMENT

The authors would like to thank the China Scholarship Council for supporting Huici Wu the international visiting at University of Waterloo, Waterloo, Canada.

REFERENCES

[1] N. Lu, N. Cheng, N. Zhang, X. Shen, and J. W. Mark, "Connected vehicles: Solutions and challenges," *IEEE Internet of Things Journal*, vol. 1, no. 4, pp. 289–299, 2014.

[2] "Cisco visual networking index: Global mobile data traffic forecast update, 2015c2020," *Cisco*, Feb. 2016.

[3] N. Zhang, N. Cheng, A. Gamage, K. Zheng, J. W. Mark, and X. Shen, "Cloud assisted hetnets toward 5G wireless networks," *IEEE Commun. Mag.*, vol. 53, no. 6, pp. 59–65, Jun. 2015.

[4] N. Zhang, S. Zhang, S. Wu, J. Ren, J. W. Mark, and X. Shen, "Beyond coexistence: Traffic steering in lte networks with unlicensed bands," *IEEE Wireless Communications*, vol. 23, no. 6, pp. 40–46, 2016.

[5] G. Yang, J. Wang, J. Luo, O. Y. Wen, H. Li, Q. Li, and S. Li, "Cooperative spectrum sensing in heterogeneous cognitive radio networks based on normalized energy detection," *IEEE Trans. Veh. Technol.*, vol. 65, no. 3, pp. 1452–1463, 2016.

[6] Y. Chen, J. Li, W. Chen, Z. Lin, and B. Vucetic, "Joint user association and resource allocation in the downlink of heterogeneous networks," *IEEE Trans. Veh. Technol.*, vol. 65, no. 7, pp. 5701– 5706, 2016.

[7] Q. Cui, H. Song, H. Wang, M. Valkama, and A. Dowhuszko, "Capacity analysis of joint transmission CoMP with adaptive modulation," *IEEE Trans. Veh. Technol.*, 2016, online published.

[8] Z. Chen, X. Hou, and C. Yang, "Training resource allocation for user-centric base station cooperation networks," *IEEE Trans. Veh. Technol.*, vol. 65, no. 4, pp. 2729–2735, 2016.

[9] D. Marabissi, G. Bartoli, R. Fantacci, and M. Pucci, "An optimized CoMP transmission for a heterogeneous network using eICIC approach," *IEEE Trans. Veh. Technol.*, vol. 65, no. 10, pp. 8230–8239, 2016.

[10] J. Zhu and H.-C. Yang, "Low-complexity QoS-aware coordinated scheduling for heterogenous networks," *IEEE Trans. Veh. Technol.*, 2016, online published.

[11] D. Lee, G. Y. Li, X.-L. Zhu, and Y. Fu, "Multi-stream multi-user coordinated beamforming for cellular networks with multiple receive antennas," *IEEE Trans. Veh. Technol.*, vol. 65, no. 5, pp. 3072–3085, 2016.

[12] G. Nigam, P. Minero, and M. Haenggi, "Spatiotemporal cooperation in heterogeneous cellular networks," *IEEE JSAC*, vol. 33, no. 6, pp. 2142–2180, Jun. 2015.

[13] M. Peng, X. Xie, Q. Hu, J. Zhang, and H. V. Poor, "Contract-based interference coordination in heterogeneous cloud radio access networks," *IEEE JSAC*, vol. 33, no. 6, pp. 1140–1153, Jun. 2015.

[14] R. Tanbourgi, S. Singh, J. G. Andrews, and F. K. Jondral, "A tractable model for noncoherent joint-transmission base station cooperation," *IEEE Trans. Wireless Commun.*, vol. 13, no. 9, pp. 4959–4973, Sep. 2014.

[15] W. Nie, F.-C. Zheng, X. Wang, W. Zhang, and S. Jin, "User-centric cross-tier base station clustering and cooperation in heterogeneous networks: Rate improvement and energy saving," *IEEE JSAC*, vol. 34, no. 5, pp. 1192–1206, May. 2016.

[16] D. Jaramillo-Ramłrez, M. Kountouris, and E. Hardouin, "Coordinated multi-point transmission with imperfect CSI and other-cell interference," *IEEE Trans. Wireless Commun.*, vol. 14, no. 4, pp. 1882–1896, Apr. 2015.

[17] A. H. Sakr and E. Hossain, "Location-aware cross-tier coordinated multipoint transmission in two-tier cellular networks," *IEEE Trans. Wireless Commun.*, vol. 13, no. 11, pp. 6311–6325, Nov. 2014.

[18] H. Wu, X. Tao, N. Li, and J. Xu, "Coverage analysis for CoMP in two-tier hetnets with nonuniformly deployed femtocells," *IEEE Commun. Lett.*, vol. 19, no. 9, pp. 1600–1603, Sep. 2015.

[19] G. Nigam, P. Minero, and M. Haenggi, "Coordinated multipoint joint transmission in heterogeneous networks," *IEEE Trans. Commun.*, vol. 62, no. 11, pp. 4134–4146, Nov. 2014.

[20] N. Yang, L. F. Wang, G. Geraci, M. Elkashlan, and J. Yuan, "Safeguarding 5G wireless communication networks using physical layer security," *IEEE Commun. Mag.*, vol. 34, no. 2, pp. 20–27, Apr. 2015.

[21] M. Conti, N. Dragoni, and V. Lesyk, "A survey of man in the middle attacks," *IEEE Commun. Surveys. Tuts.*, vol. 18, no. 3, pp. 2027–2051, 2016.

[22] A. Wasef, R. Lu, X. Lin, and X. Shen, "Complementing public key infrastructure to secure vehicular AD HOC networks," *IEEE Wireless Commun.*, vol. 17, no. 5, pp. 22–28, 2010.

[23] M. Haenggi, "Mean interference in hard-core wireless networks," *IEEE Commun. Lett.*, vol. 15, no. 8, pp. 792–794, Aug. 2011.

[24] A. M. Ibrahim, T. ElBatt, and A. El-Keyi, "Coverage probability analysis for wireless networks using repulsive point processes," 2013 IEEE 24th International Symposium on Personal Indoor and Mobile Radio Communications (PIMRC). IEEE, Sept. 2013, pp. 1002–1007.

[25] M. Haenggi, *Stochastic Geometry for Wireless Networks*. Cambridge University Press, 2012.

[26] N. Jindal, J. G. Andrews, and S. Weber, "Multi-antenna communication in Ad hoc networks: Achieving MIMO gains with SIMO transmission," *IEEE Trans. Commun.*, vol. 59, no. 2, pp. 529–540, Frb. 2011.

[27] C. Li, J. Zhang, J. G. Andrews, and K. B. Letaief, "Success probability and area spectral efficiency in multiuser MIMO hetnets," *IEEE Trans. Commun*, vol. 99, no. pp, p. Online Published, Mar. 2016.

[28] A. Mukherjee, S. A. A. Fakoorian, J. Huang, and A. L. Swindlehurst, "Principles of physical layer security in multiuser wireless networks: A survey," *IEEE Communications Surveys & Tutorials*, vol. 16, no. 3, pp. 1550–1573, 2014.

[29] A. Guo, Y. Zhong, W. Zhang, and M. Haenggi, "The gausscpoisson process for wireless networks and the benefits of cooperation," *IEEE Trans. Commun.*, vol. 64, no. 5, pp. 1916–1929, May 2016.

[30] R. Heath, T. Wu, Y. H. Kwon, and A. Soong, "Multiuser MIMO in distributed antenna systems with out-of-cell interference," *IEEE Trans. Commun*, vol. 59, no. 10, pp. 4885–4899, Oct. 2011.

[31] K. Hosseini, W. Yu, and R. Adve, "Large-scale MIMO versus network mimo for multicell interference mitigation," *IEEE J. Sel. Topics Signal Process.*, vol. 8, no. 5, pp. 930–941, Oct. 2014.

[32] N. Zhang, N. Cheng, N. Lu, H. Zhou, J. W. Mark, and X. Shen, "Risk-aware cooperative spectrum access for multi-channel cognitive radio networks," *IEEE JSAC*, vol. 32, no. 3, pp. 516–527, 2014.

[33] T. H. Noor, Q. Z. Sheng, L. Yao, S. Dustdar, and A. H. Ngu, "Cloudarmor: Supporting reputation-based trust management for cloud services," *IEEE Trans. Parallel. Distributed Systems*, vol. 27, no. 2, pp. 367–380, 2016.

[34] L. Wei, H. Zhu, Z. Cao, and X. S. Shen, "Mobiid: A user-centric and social-aware reputation based incentive scheme for delay/disruption tolerant networks," *Ad-hoc, Mobile, and Wireless Networks, ser. Lecture Notes in Computer Science, H. Frey, X. Li, and S. Ruehrup, Eds. Springer Berlin / Heidelberg*, vol. 6811, pp. 177–190, 2011.

[35] K. A. Hamdi, "A useful lemma for capacity analysis of fading interference channels," *IEEE Trans. Commun.*, vol. 58, no. 2, pp. 411–416, Feb. 2010.

[36] S. Gradshteyn and I. M. Ryzhik, *Table of Integrals, Series, and Products*. 6th edition, New York: Academic Press, 2000.

This article has been accepted for publication in a future issue of this journal, but has not been fully edited. Content may change prior to final publication. Citation information: DOI 10.1109/TVT.2017.2729346, IEEE Transactions on Vehicular Technology

Huici Wu received her B.S. degree in Information Engineering School from Communication University of China, Beijing, China, in 2013. She is currently pursuing Ph.D. degree with the communications and information systems at Beijing University of Posts and Telecommunications, Beijing, China. From September 2016 to August 2017, she is visiting the Broadband Communications Research (BBCR) Group, Department of Electrical and Computer Engineering, University of Waterloo, Waterloo, ON, Canada. Her research interests are in the area of wireless communications and networks, with current emphasis on the cooperation and physical layer security in heterogeneous networks.

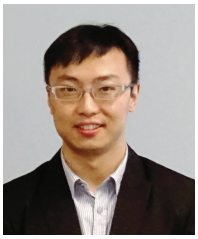

Ning Zhang (M'15) received the Ph.D degree from University of Waterloo in 2015. He is now an assistant professor in the Department of Computing Science at Texas A&M University-Corpus Christi. Before that, he was a postdoctoral research fellow at BBCR lab in University of Waterloo. He was the co-recipient of the Best Paper Award at IEEE GLOBECOM 2014 and IEEE WCSP 2015. His current research interests include next generation wireless networks, software defined networking, vehicular networks, and physical layer security.

Xiaofeng Tao (SM'13) received the B.S. degree in electrical engineering from Xian Jiaotong University, Xian, China, in 1993 and the M.S.E.E. and Ph.D. degrees in telecommunication engineering from the Beijing University of Posts and Telecommunications (BUPT), Beijing, China, in 1999 and 2002, respectively.

He was a Visiting Professor with Stanford University, Stanford, CA, USA, from 2010 to 2011; the Chief Architect of the Chinese National FuTURE Fourth-Generation (4G) TDD working group from 2003 to 2006; and established the 4G TDD CoMP trial network in 2006. He is currently a Professor with the BUPT and a Fellow of the Institution of Engineering and Technology. He is the inventor or coinventor of 50 patents and the author or coauthor of 120 papers in 4G and beyond 4G.

Zhiqing Wei (S'13-M'15) received the B.S. and Ph.D. degrees from Beijing University of Posts and Telecommunications (BUPT) in 2010 and 2015 respectively. Now he is a lecture at BUPT. His research interests are network information theory and optimization of wireless networks such as cognitive radio networks, robotic networks, etc.

Xuemin (Sherman) Shen (M'97-SM'02-F'09) received the B.Sc.(1982) degree from Dalian Maritime University (China) and the M.Sc. (1987) and Ph.D. degrees (1990) from Rutgers University, New Jersey (USA), all in electrical engineering. He is a University Professor and the Associate Chair for Graduate Studies, Department of Electrical and Computer Engineering, University of Waterloo, Canada. Dr. Shens research focuses on resource management, wireless network security, social networks, smart grid, and vehicular ad hoc and sensor networks. He was an elected member of IEEE ComSoc Board of Governor, and the Chair of Distinguished Lecturers Selection Committee. Dr. Shen served as the Technical Program Committee Chair/Co-Chair for IEEE Globecom16, Infocom14, IEEE VTC10 Fall, and Globecom07, the Symposia Chair for IEEE ICC10, the Tutorial Chair for IEEE VTC11 Spring and IEEE ICC08, the General Co-Chair for ACM Mobihoc15, Chinacom07 and QShine06, the Chair for IEEE Communications Society Technical Committee on Wireless Communications, and P2P Communications and Networking. He also serves/served as the Editor-in-Chief for IEEE Internet of Things Journal, IEEE Network, Peer-to-Peer Networking and Application, and IET Communications; a Founding Area Editor for IEEE Transactions on Wireless Communications; an Associate Editor for IEEE Transactions on Vehicular Technology, Computer Networks, and ACM/Wireless Networks, etc.; and the Guest Editor for IEEE JSAC, IEEE Wireless Communications, IEEE Communications Magazine, and ACM Mobile Networks and Applications, etc. Dr. Shen received the Excellent Graduate Supervision Award in 2006, and the Premiers Research Excellence Award (PREA) in 2003 from the Province of Ontario, Canada. Dr. Shen is a registered Professional Engineer of Ontario, Canada, an IEEE Fellow, an Engineering Institute of Canada Fellow, a Canadian Academy of Engineering Fellow, a Royal Society of Canada Fellow, and a Distinguished Lecturer of IEEE Vehicular Technology Society and Communications Society.